

High-saturated-fat diet induces gestational diabetes and placental vasculopathy in C57BL/6 mice

Chengya Liang^a, Kristi DeCourcy^b, Mary R. Prater^{a,c,*}

^aVA-MD Regional College of Veterinary Medicine, Virginia Tech, Blacksburg, VA 24061, USA

^bFralin Life Science Institute, Virginia Tech, Blacksburg, VA 24061, USA

^cEdward Via Virginia College of Osteopathic Medicine, Blacksburg, VA 24060, USA

Received 25 August 2009; accepted 19 October 2009

Abstract

Gestational diabetes mellitus (GDM) is a commonly encountered disorder of mid to late pregnancy that is characterized by hyperglycemia, hyperinsulinemia, and impaired glucose tolerance. Gestational diabetes mellitus is thought to be multifactorial in origin and derives from both genetic and environmental factors. However, the mechanisms underlying GDM are incompletely understood; and current GDM animal models do not appear to closely mimic the clinical situation in humans. The present study used environmental exposure to high-saturated-fat diet (HFD) in an effort to develop a GDM mouse model that closely simulates metabolic abnormalities seen in human GDM. This model was then used to determine the contributions of HFD-induced placental oxidative stress (OS) and vascular dysregulation, which are observed in GDM patients and are believed to contribute to the pathogenesis of the disease. Pathologic manifestations of the disease were quantified by evaluating the extent of placental lipid peroxidation and by determining protective effects of dietary antioxidant quercetin supplementation to reduce HFD-associated placental OS. In this study, female C57BL/6 mice were fed HFD for 1 month before conception and throughout gestation to mimic chronic maternal fast food consumption. Maternal body weight increased from gestation day (GD) 0 to GD19 by 41% with HFD, as compared with 23% in control dams; HFD dams also developed insulin resistance (66% increase in plasma insulin and 27% increase in plasma glucose levels by GD10) as compared with control dams. Placentas from HFD GD19 dams demonstrated loss of trophoblasts and OS-mediated labyrinthine endothelial cellular damage, the latter of which was prevented with quercetin supplementation. Our findings suggest that prenatal HFD alters glucose metabolism and elevates placental OS, which are believed to collectively relate to improper formation of the conceptus and impaired birth outcome.

© 2010 Elsevier Inc. All rights reserved.

1. Introduction

Gestational diabetes mellitus (GDM) is characterized by hyperglycemia, hyperinsulinemia, and insulin resistance, as well as placental and fetal maldevelopment [1]. Approximately 2% to 10% of all pregnancies are affected by GDM, and those mothers who experience GDM demonstrate elevated long-term risk of type 2 diabetes mellitus later in life [1]. Genetic predisposition and pregnancy hormones are

thought to collectively contribute to the pathogenesis of this disease by increasing insulin resistance, causing β -cell dysfunction, and reducing insulin-mediated glucose transport [2,3]. However, recent studies show that genetic and hormonal factors are unable to fully explain development of GDM. As such, other environmental factors, such as high-saturated-fat diet (HFD), may enhance glucose intolerance during pregnancy by reducing insulin-mediated glucose transport in muscle and adipose tissue, and promote insulin resistance and obesity in pregnancy [4]. Consumption of HFD increases oxidative stress (OS) and adversely affects endocrine homeostasis, resulting in poorly controlled hyperglycemia, hyperinsulinemia, and insulin resistance [4]. Consumption of HFD during pregnancy may also elevate risk of GDM through similar mechanisms, and this theory was investigated in the present proposal.

Conflicts of interest: No conflicts of interest related to this manuscript.

* Corresponding author. Edward Via Virginia College of Osteopathic Medicine, Blacksburg, VA, 24060, USA. Tel.: +1 540 231 3996; fax: +1 540 231 5252

E-mail address: mrprater@vt.edu (M.R. Prater).

Human GDM is associated with placental endothelial dysfunction that impairs gas and nutrient transfer to the fetus [5]; these changes are thought to be in part mediated by elevated placental OS or antioxidant depletion. Increased production of reactive oxygen species (ROS) in pregnancy is thought to be caused in large part by increased oxygen intake due to high tissue demands, which results in mitochondrial dysfunction. Oxidative stress may be further exacerbated by toxic substances, smoking, asphyxia, and consumption of an HFD. Fatty acid consumption is thought to decrease formation of superoxide dismutase, increase production of superoxide by the mitochondrial electron-transport chain, and generate excess ROS that damage cell membranes [6]. Diabetic and preeclamptic women exhibit placental vascular damage due to increased superoxide, which underscores the importance of mitigating OS to improve pregnancy outcome [7]. Quercetin (Q) is a potent flavonoid antioxidant that is commonly found in fresh fruits and vegetables. It contains 2 antioxidant pharmacophores that efficiently scavenge free radicals [8]. Oral administration of Q is readily absorbed by enterocytes, has a relatively long elimination half-life (between 11 and 22 hours), and can readily pass through the placenta, thus affecting both fetus and placenta [9]. In this study, antioxidant effects of Q against HFD-induced manifestations of GDM were examined.

Animal models of diabetes during pregnancy are crucial to explore the pathophysiologic aspects of human GDM. Although there are several animal models (genetic and chemically induced) available for the study of GDM, none closely mimic the pattern of disease initiation and development seen in the clinical situation in humans. The nitrosourea streptozotocin induces high hyperglycemia and hypoinsulinemia by destruction of pancreatic β -cells, which more closely approximates type 1 diabetes mellitus than GDM [10,11]. Low-dose streptozotocin induces moderate, but unpredictable, hyperglycemia [12–14]. Transgenic GDM animal models develop hyperglycemia similarly to human GDM [15], but human GDM patients do not express the gene alterations that cause hyperglycemia in these knockout strains [16,17].

The present study endeavors to develop a GDM mouse model that closely simulates the common metabolic abnormalities of human GDM, using HFD, and to explore pathophysiologic mechanisms linking gestational HFD to elevated OS, insulin resistance, and placental vasculopathy.

2. Materials and methods

2.1. Animals and diet

Six-week-old C57BL/6J mice were obtained from Jackson Laboratories (Bar Harbor, ME). Mice were acclimated in groups of 5 as such: fresh food and water ad libitum, temperature ($22.0^{\circ}\text{C} \pm 1^{\circ}\text{C}$), humidity (40%–60%), and light (12-hour/12-hour light/dark) for 2 weeks. Experiments were approved by the Virginia Tech Animal Care and

Use Committee and not initiated until approval was granted. Female mice were arbitrarily assigned to 1 of 3 groups: control, HFD, or HFD + Q, in a generalized randomized complete block design, with 16 mice per group. Mice were fed control rodent diet (Global Diet 2018: 18% protein, 5% fat; Harlan Teklad, Madison, WI), HFD (20% protein, 60% total fat, 32.1% saturated fat; Research Diets, New Brunswick, NJ) (Table 1), or HFD supplemented with 66 mg/kg Q (HFD/Q). This level of Q supplementation approximates a typical daily human Q consumption of 700 mg/d, given an average daily consumption of 5g food per mouse per day [18]. After 1-month dietary intervention, breeding was conducted overnight in a 1:2 ratio; mating was confirmed by presence of a vaginal mucous plug the following morning, which represented gestation day (GD) 0.

2.2. Body weight, blood glucose, and plasma insulin

Female body weight, blood glucose, and plasma insulin were recorded before dietary intervention; after 4 weeks of HFD; and at GD0, 10, and 19. Body weight was recorded on a top-loading balance (Accu-622; Fisher Scientific, Suwanee, GA), and nonfasting maternal blood samples were obtained via tail venipuncture to determine insulin and glucose levels. Blood glucose levels were determined by glucometer (LifeScan Surestep; Johnson & Johnson, Langhorne, PA) and plasma insulin levels were quantified by enzyme-linked immunosorbent assay (ELISA; Alpco Diagnostics, Salem, NH) according to the manufacturer's instructions.

2.3. Placental weight

Dams were euthanized on GD19 by intraperitoneal injection of sodium pentobarbital (150 mg/kg), and placentas were immediately collected. Placental weights were recorded as average individual placental wet weights per litter on a top-loading balance. Placentas were reserved for histopathologic analysis, quantification of OS, and immunofluorescent staining of labyrinthine endothelial cells.

2.4. Histopathology

A portion of GD19 placentas from each group was preserved in Bouin fixative for 18 hours, washed with 10 vol ddH₂O, and stored in 70% EtOH. Placentas were transected perpendicular to the long axis of the disc,

Table 1
Composition of the HFD

High-fat diet	g %	kcal %
Protein	26.2	20
Carbohydrate	26.3	20
Fat	34.9	60
Fat composition		%
Saturated		32.1
Monounsaturated		43
Polyunsaturated		16.9

processed, and paraffin embedded; and 5- μ m sections were stained with hematoxylin-eosin (H&E) for morphologic analysis by light microscopy. Viable trophoblasts at 1000 \times magnification were enumerated (average 10 representative microscopic fields). In addition, nonviable labyrinthine endothelial cells from control and treatment placentas were enumerated at 400 \times magnification (average 10 representative microscopic fields). Placentas from all groups were also observed for overall evidence of necrosis, inflammation, hemorrhage, and fibrosis.

2.5. Placental OS

A second portion of GD19 placentas from all groups was stored at -70°C for measurement of malondialdehyde (MDA), a common stable marker for OS-induced lipid peroxidation. The degree of lipid peroxidation per milligram total protein was measured (using BCA protein assay kit; PIERCE, Rockford, IL, and Bioxytech MDA-586; Oxis Research, Portland, OR). Briefly, placentas from each group were homogenized in 0.1 mol/L phosphate-buffered saline (PBS) and 0.5 mol/L butylated hydroxytoluene. Samples (200 μL) were added to 640 μL of *N*-methyl-2-phenylindole, vortexed, and then mixed with 150 μL of concentrated HCl before incubation at 45°C for 60 minutes. The turbid samples were centrifuged for 10 minutes at 10 000g; absorbance of supernatant was measured at 586 nm (Beckman DU-640 spectrophotometer; International MI-SS, Corona, CA).

2.6. Immunofluorescence

A third portion of GD19 Bouin-fixed placentas from each group was processed, paraffin embedded, and sectioned at 5 μm for CD31 immunofluorescence and confocal microscopic evaluation. Placentas were deparaffinized in xylene and rehydrated in serial alcohol solutions. Tissues were dipped in unmasking solution (Vector Laboratories, Burlingame, CA) at 120°C in a pressure cooker for 5 minutes and washed 3 times in 0.1 mol/L PBS for 5 minutes. Placental sections were then blocked in 10% rabbit serum (Fisher Scientific) for 30 minutes followed by incubation in CD31 1 $^{\circ}$ antibody (M-20; Santa Cruz Biotechnology, Santa Cruz, CA) diluted 1:300 in 1.5% serum overnight at 4°C . The following day, the slides were washed 3 times for 10 minutes each in 0.1 mol/L PBS followed by incubation for 30 minutes in Alexa Fluor 594 rabbit anti-goat antibody (Invitrogen, Carlsbad, CA) diluted 1:200 in 0.1 mol/L PBS. After several washes in 0.1 mol/L PBS, slides were mounted using mounting solution with DAPI (Vector Laboratories) and visualized under confocal laser scanning microscopy (Zeiss CLSM 510 META; Carl Zeiss Microimaging GmbH, Gottingen, Germany).

2.7. Statistical analysis

All data were presented as mean \pm standard error. One-way analysis of variance was used with Tukey-Kramer honestly significant difference test (JMP; SAS Institute, Cary, NC) to

establish significant differences between groups. Data were determined to be statistically different when $P < .05$.

3. Results

3.1. Blood glucose and plasma insulin

Blood glucose levels were determined before and after HFD feeding and at GD0, 10, and 19 for all groups, and showed a progressive increase at the end of HFD feeding and during pregnancy in HFD but not control or HFD/Q groups

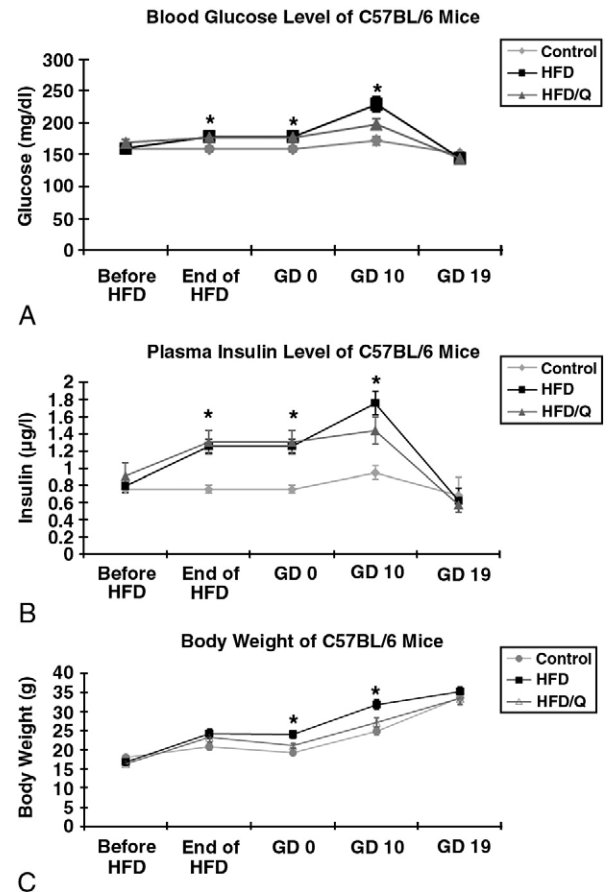


Fig. 1. A, Blood glucose levels of C57BL/6 mice. Blood glucose concentrations were measured before HFD, at the end of 4 weeks of HFD, and during pregnancy (GD0, 10, and 19) in control, HFD, and HFD/Q groups. The HFD group showed significantly higher blood glucose levels as compared with control dams. The HFD/Q group was not significantly different than HFD or controls. Values are given as means \pm SEM. *Significant difference, $P < .05$. B, Plasma insulin levels of C57BL/6 mice. Plasma insulin concentrations were measured by ELISA before, after 4 weeks of HFD, and during pregnancy (GD0, 10, and 19). Mice in HFD group became significantly hyperinsulinemic as compared with controls. Quercetin supplementation was not significantly protective against HFD-induced hyperinsulinemia. Values are given as means \pm SEM. *Significant difference, $P < .05$. C, Effect of HFD on maternal body weight. Female body weight was measured before HFD, at the end of 4 weeks of HFD, and during pregnancy (GD0, 10, and 19). The HFD-treated mice weighed significantly more than the controls on GD0 and GD10. Body weight of mice in the HFD/Q group was not significantly different as compared with that of HFD dams. Values are given as means \pm SEM. *Significant difference, $P < .05$.

(Fig. 1A). Blood glucose peaked at 229.3 mg/dL on GD10 and decreased by GD19 in the HFD group, and at 172.4 mg/dL at GD10 in controls. The blood glucose level from HFD/Q group did not differ from controls. Plasma insulin levels were measured by ELISA at the same time points in all groups, and increased at the end of HFD feeding by 58.3% in the HFD group and continued to increase throughout pregnancy; controls did not increase during this period (Fig. 1B), and Q did not protect against HFD-associated hyperinsulinemia. Together, Fig. 1A and B demonstrate a parallel pattern of modification of prenatal blood glucose and plasma insulin levels, and suggest insulin resistance in the HFD and HFD/Q groups.

3.2. Body weight

Maternal body weight was determined at the same time points as described above (Fig. 1C). Control maternal body weight moderately increased throughout the pregnancy, from a mean of 17.5 g before feeding trial to 19 g at GD0, 24.6 g at GD10, and 34.8 g at GD19. In contrast, HFD dams rapidly increased in body weight, from 23.5 g at GD0 to 32 g at GD10 and 36.1 g at GD19. The HFD dam weight was significantly increased as compared with that of controls and HFD/Q at GD0 and 10, but not at GD19, perhaps because of late-gestation lipolytic alterations in placental growth hormone metabolism.

3.3. Placental histopathology

Placentas from GD19 dams of each treatment group were evaluated by light microscopy for alterations in architecture across treatment groups using 5- μ m H&E sections (Fig. 2). Placentas from HFD-treated dams (Fig. 2B) visually displayed multifocal areas of hemorrhagic fibrinous necrosis and mixed inflammation that predominated in the labyrinthine layer, with karyolysis and pyknosis, cellular fragmentation, and hypereosinophilia, which are key indicators of cellular necrosis. The trophoblastic cell layer appeared to display a relative paucity of trophoblasts (Fig. 2B), whereas control (Fig. 2A) and HFD/Q (Fig. 2C) trophoblast placentas appeared highly cellular, with minimal evidence of labyrinthine necrosis, inflammation, or hemorrhage. This visual inspection of HFD-induced placental alterations was followed by efforts to quantify these treatment-associated observed differences. Consequently, trophoblastic and labyrinthine layers were inspected separately and evaluated for average number of trophoblasts per 1000 \times magnification field (average of 10 representative fields of spongiotrophoblast) and average number of nonviable labyrinthine endothelial cells per 400 \times magnification field (average of 10 representative fields of labyrinthine placenta), respectively. Spongiotrophoblast examination revealed a significantly reduced average number of viable trophoblast cell numbers (53.40 per 1000 \times magnification field compared with 69.73/field in control spongiotrophoblast, Fig. 3A). Concurrent Q did not protect against HFD-associated loss of

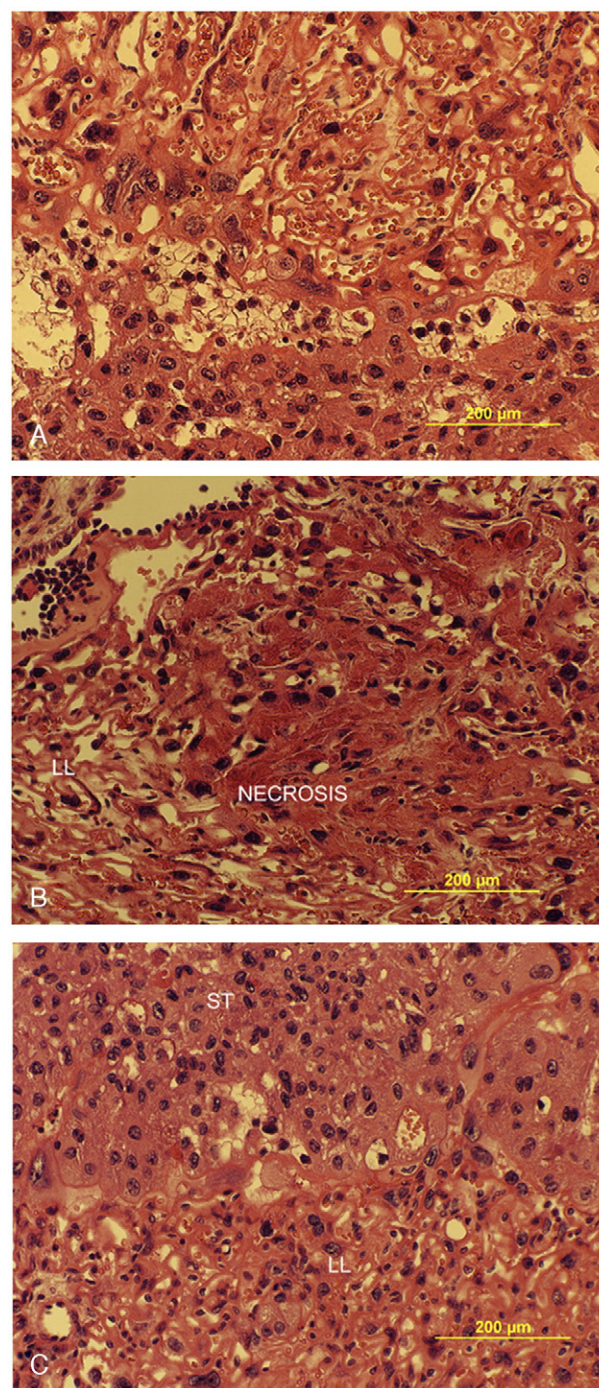


Fig. 2. Histopathologic images of GD19 mouse placentas. The GD19 placentas were stained with H&E for morphologic analysis under light microscopy. A, Control GD19 placenta was highly cellular, with minimal evidence of necrosis, inflammation, or hemorrhage. B, HFD GD19 placenta showed multifocal areas of fibrinonecrosis, cellular fragmentation, and hypereosinophilia, which predominately targeted endothelium in the labyrinthine layer. The trophoblast cell layer displayed reduced cellularity as compared with controls. C, HFD/Q GD19 placenta was highly cellular, with minimal evidence of necrosis, inflammation, or hemorrhage, which was comparable to controls. LL indicates labyrinthine layer; ST, spongiotrophoblast.

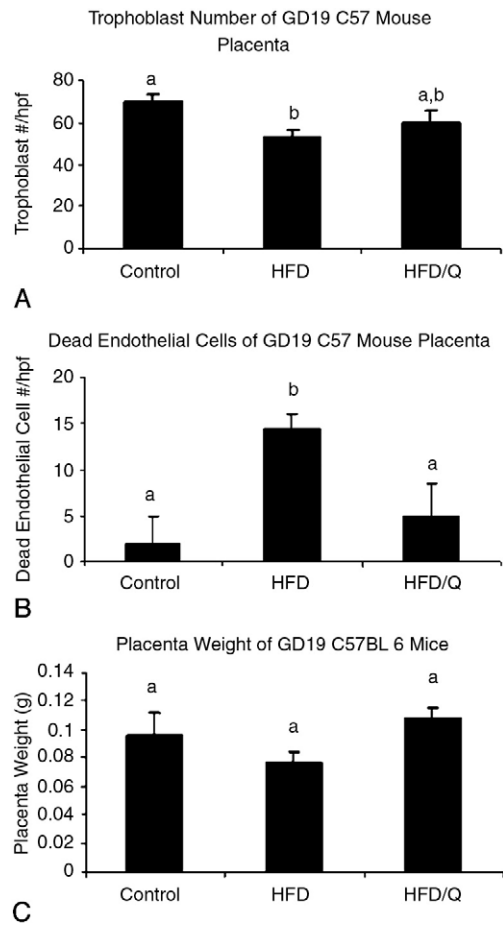


Fig. 3. A, Trophoblast numbers in GD19 C57BL/6 mouse placentas. Trophoblast health was evaluated by enumeration of viable trophoblasts in 10 fields of 1000 \times magnification. The HFD group showed significantly fewer viable trophoblast cells than controls. Quercetin did not significantly protect against trophoblast loss. Values are given as means \pm SEM. Bars with different letters are significantly different, $P < .05$. B, Endothelial cell necrosis in GD19 C57BL/6 mouse placentas. Nonviable labyrinthine endothelial cells from different dams were enumerated in 10 fields of 400 \times magnification. The HFD group displayed significantly increased necrotic endothelial cells as compared with controls. Quercetin supplementation showed protective effects against HFD-associated labyrinthine endothelial cell loss. Values are given as means \pm SEM. Bars with different letters are significantly different, $P < .05$. C, Placental weight of GD19 mice. Placental weights were measured immediately after euthanasia. Neither HFD nor Q affected placental wet weight. Values are given as means \pm SEM. Bars with same letters are not significantly different, $P > .05$.

trophoblast, which suggested that OS was not the primary mechanism of trophoblast cellular loss. Labyrinthine placentas from gestational HFD dams displayed significantly increased necrosis of labyrinthine endothelial cells (average of 14.48 necrotic cells per ten 400 \times magnification fields, as compared with 1.87 in control placentas; Fig. 3B). Quercetin was protective against HFD-induced endothelial cell loss and significantly decreased endothelial necrosis to 5 per 400 \times magnification field, suggesting that changes in labyrinthine placenta may have resulted from HFD-induced elevations in OS (Fig. 3B). These changes were accompanied by an insignificant loss in GD19 HFD dam placental weight (78%

of controls, Fig. 3C). The HFD/Q placental weight was also not different from that of controls.

3.4. Placental OS

Maternal dietary Q reduced labyrinthine placental necrotic lesions, which anecdotally suggested OS-mediated disruption of late-gestation placental health. To more precisely quantify OS-mediated placental damage, GD19 placentas from all groups were evaluated for levels of the lipid peroxidation product MDA. Results of this study determined that HFD dams showed increased MDA levels as compared with controls, suggesting increased lipid peroxidation and elevated OS due to gestational dietary HFD (Fig. 4). Quercetin supplementation decreased placental MDA levels, which supported the hypothesis that HFD causes OS-mediated lesions and touted beneficial antioxidant effects of Q against HFD-induced labyrinthine placental vascular damage. These data supported the cellular changes observed via histopathologic examination of GD19 placentas in this study.

3.5. CD31 immunofluorescence

CD31 immunofluorescent staining intensity was evaluated in GD19 placentas. Placentas from HFD dams (Fig. 5A, panel b) showed decreased overall levels of CD31 immunostaining intensity of labyrinthine endothelium as compared with control (A), which indicate endothelial necrosis and placental cellular and vascular pathology secondary to gestational HFD. Placenta from HFD/Q dams (C) showed near-control intensity of CD31 immunostaining, demonstrating antioxidant protection of labyrinthine vascular integrity. High-magnification CD31 immunostaining intensity of labyrinthine layer capillaries from control (Fig. 5B, panel a), HFD (B), and HFD/Q (C) placentas showed markedly stronger CD31 staining intensity in control vs HFD labyrinthine capillaries. Capillary CD31 immunofluorescent staining in HFD/Q labyrinthine placenta was comparable to controls, providing a potential mechanistic explanation that

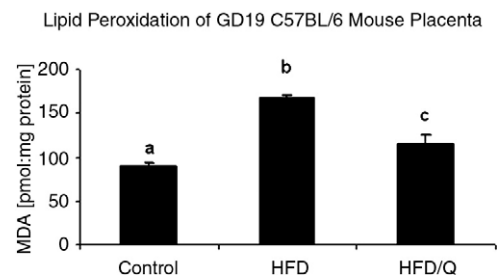


Fig. 4. Lipid peroxidation of GD19 C57BL/6 mouse placentas. Malondialdehyde levels were evaluated in GD19 placenta from each group as a measurement of placental OS. The HFD group demonstrated significantly higher MDA levels as compared with controls, indicating HFD-associated elevated placental OS. Quercetin supplementation significantly reduced placental lipid peroxidation. Values are given as means \pm SEM. Bars with different letters are significantly different, $P < .05$.

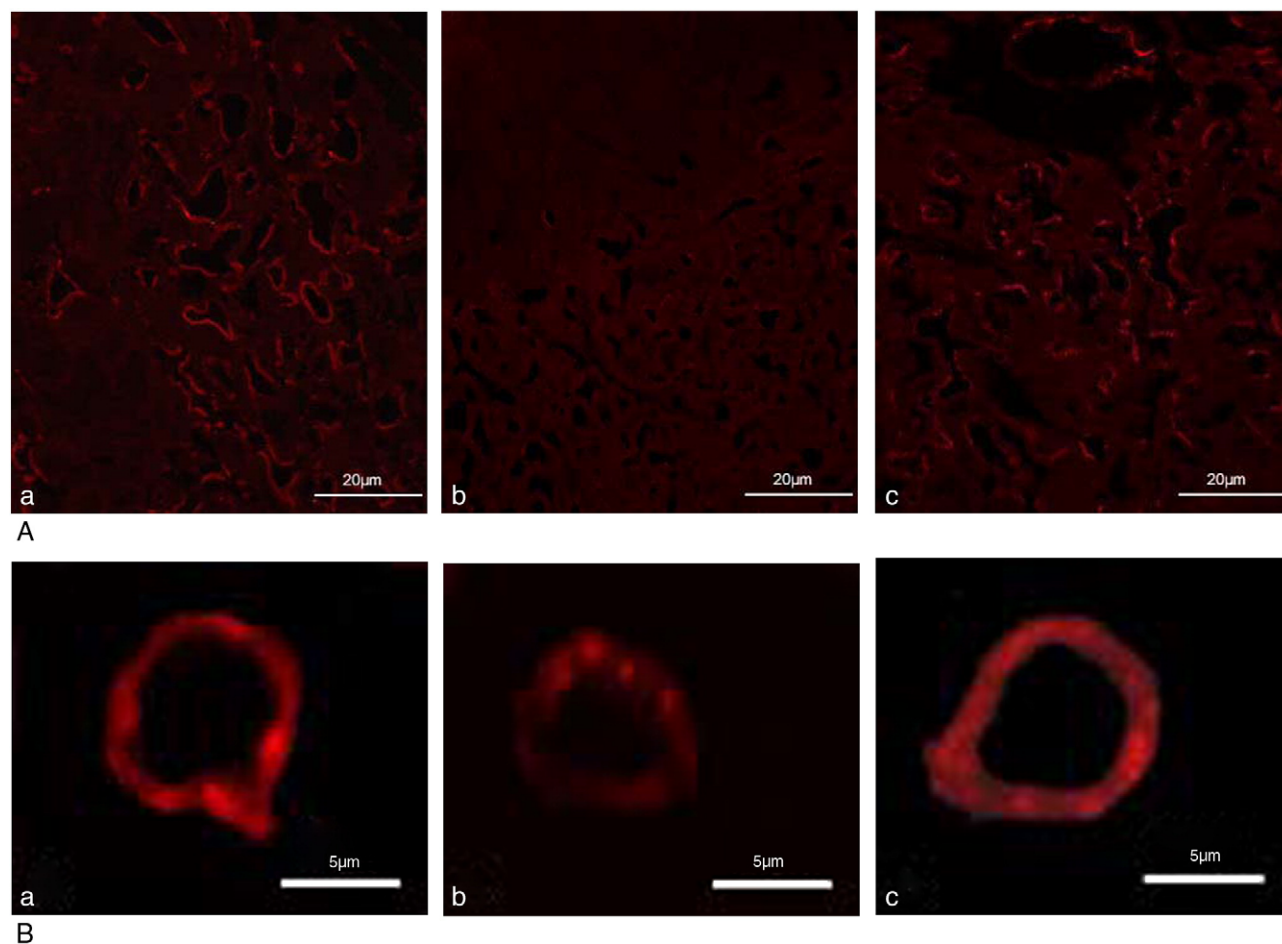


Fig. 5. A, CD31 immunofluorescence staining of GD19 mouse placenta. CD31 immunofluorescently stained placentas from control, HFD, and HFD/Q groups were observed via confocal microscopy. Placentas from control dams showed visibly stronger CD31 staining intensity (a) as compared with HFD placentas, which were largely devoid of CD31 labyrinthine endothelial cell staining (b). Placenta from HFD/Q (c) dams exhibited near-control level CD31 staining intensity. B, CD31 immunofluorescence staining of GD19 mouse labyrinthine placenta capillary endothelium. Control labyrinthine placental capillary endothelium displayed high intensity CD31 staining (a) as compared with HFD labyrinthine placental capillary endothelium (b). The HFD labyrinthine placental capillary endothelial cells showed dramatically decreased CD31 staining intensity; and concurrent Q supplementation exhibited near-control level CD31 immunofluorescence staining (c), suggesting possible protective effects of antioxidant supplementation against HFD-induced labyrinthine placental vasculopathy.

Q supplementation protects against HFD-elevated OS and labyrinthine placental damage.

4. Discussion

The present study demonstrated that diets rich in saturated fats before and during pregnancy may result in pathologic manifestations in mice similar to the human condition of GDM. This dietary intervention elevated midgestational body weight, insulin resistance, placental OS, and placental vasculopathy, which together are thought to contribute to adverse consequences of fetal development and impaired birth outcome. Maternal hyperglycemia, hyperinsulinemia, and insulin resistance were observed in the present study after 4-week HFD before breeding and throughout pregnancy, suggesting that chronic HFD, which approximates the

macronutrient content of fast food, increases plasma free fatty acid (FFA) concentrations and induces an insulin-resistant state that results in obesity and non-insulin-dependent diabetes [19–21]. Elevated plasma FFA levels in humans cause insulin resistance by inhibiting glucose transport and/or phosphorylation activity and reducing the rate of both muscle glycogen synthesis and glucose oxidation [22]. Studies show that preferential use of increased fatty acids for oxidation blunts insulin-mediated reduction of hepatic glucose output and reduces glucose uptake or utilization in skeletal muscle leading to compensatory hyperinsulinemia, a common feature of insulin resistance [23–25]. Our study suggests that the dynamic relationship between insulin resistance and compensatory increases in β -cell glucose metabolism was disrupted by HFD, causing β -cell compensation to fail, glucose levels to rise, and impaired glucose tolerance.

Our discovery of a possible link between HFD and insulin production offers new information that may improve understanding of etiopathogenic mechanisms triggering early stages of GDM. Ohtsubo et al [26] found that HFD suppresses activity of pancreatic *Mgat4a*-encoded GlcNAcT-IV glycosyltransferase and leads to type 2 diabetes mellitus in mice due to failure of pancreatic β -cells. GlcNAcT-IV glycosyltransferase normally maintains glucose transporters on the surface of pancreatic β -cells, such as glucose transporter 2. Glucose transporter 2 plays a crucial role in allowing β -cells to sense circulating glucose levels and in the transport of glucose into pancreatic β -cells, which then triggers insulin secretion. Results of the present study may suggest GlcNAcT-IV glycosyltransferase or glucose transporter 2 dysfunction; additional studies are now required to explore this pathophysiologic mechanism of HFD-induced insulin resistance.

In this study, placental OS and labyrinthine placental endothelial damage were increased with HFD feeding before and throughout gestation, similar to human GDM. In human GDM, increased blood glucose is accompanied by either reduced superoxide dismutase production [27] or overproduction of ROS such as superoxide by the mitochondrial electron-transport chain, which results in vascular complications and DNA damage associated with embryonic dysmorphogenesis [28]. This serves as a plausible etiopathologic mechanism of placental vascular damage in human GDM and our GDM mouse model. Elevated placental OS, blood glucose, and plasma insulin due to increased plasma FFA concentration secondary to HFD likely resulted in diminished placental blood flow, disrupted labyrinthine endothelium, and vasculopathy, similar to what has been reported in the human literature [29]. In this study, we also observed a trend of decreased placental weight in HFD group caused by OS-induced trophoblast loss and endothelial necrosis. Results of placental histopathology, MDA measurement, and CD31 immunofluorescent staining data further demonstrated that OS-induced vasculopathy of placenta may significantly contribute to symptoms of GDM of C57BL/6 mice. CD31, or platelet-endothelial cell adhesion molecule-1, is an integral membrane glycoprotein found at endothelial intercellular junctions that is involved in angiogenesis and wound healing and is a commonly used biomarker of endothelial viability. Decreased expression of CD31 indicates endothelial dysfunction and vasculopathy [30]. Reduced placental CD31 has been suggested to be a reliable biomarker for OS-mediated reduction of trophoblast invasion, as in preeclampsia [31]. CD31 immunofluorescent staining intensity was evaluated in GD19 placentas in an effort to mechanistically explain a link between HFD, elevated OS, and reduced placental functionality to support proper fetal development. Our research suggested that HFD treatment decreased CD31 staining intensity of labyrinthine placental capillary endothelium, which further supported histologic evidence of vascular damage associated with HFD during pregnancy.

It is noted that despite significantly increased maternal body weight during pregnancy and clinical signs of GDM associated with HFD, GD19 fetuses from HFD dams were not macrosomic, as might be expected with maternal overnutrition and hyperglycemia, and in fact were slightly lighter than control fetuses [32]. This apparently unexpected finding is easily explainable by understanding that murine pancreatic insulin-producing capacity matures postnatally, in contrast to human fetuses whose β -cells are fully functional prenatally; because maternal insulin cannot cross placenta but glucose can, human fetuses respond to maternal overnutrition through insulin-mediated glucose uptake and accelerated growth, whereas fetal mice respond less exquisitely to maternal glucose [33]. Consequently, we believe that our fetuses may have responded more exquisitely to the HFD-induced OS and placental insufficiency, rather than the GDM-associated hyperglycemia and overnutrition. In addition, microcomputed tomographic image analysis of GD19 fetuses from HFD dams revealed significant delay of fetal skeletal development associated with OS-mediated dysregulation of osteogenic signaling [32]. According to the Barker theory, the “developmental origins of health and disease,” poor gestational environment causes epigenetic changes in fetal programming that cause small-for-gestational-age neonates and permanently altered phenotype. These offspring also exhibit elevated risk of adult-onset skeletal, metabolic, and endocrine diseases because of postnatal “catch-up growth” and are at higher risk for type 2 diabetes mellitus, obesity, hypertension, and osteoporosis because of permanently altered signaling pathways during fetal life [34,35]. These findings collectively suggest the importance of proper prenatal nutrition in proper birth outcome and long-term good health.

Quercetin is a potent ROS scavenger that is ubiquitously found in fruits and vegetables and is a common nutritional supplement [36]. Studies show that Q is absorbed from the diet as glycosides, and it is detected in plasma from nonsupplemented humans at individual levels in the range of 0.5 to 1.6 $\mu\text{mol/L}$ [37]. Quercetin is thought to convey beneficial health effects, partly via antioxidant protection of cellular components against ROS [38]. Quercetin readily passes through the placenta and, as such, may influence fetal development both indirectly (placental effects of Q exposure) and directly (transplacental Q delivery) after maternal Q ingestion [9]. Our laboratory's previous studies show that Q protects against fetal and placental pathologies induced by methylnitrosourea [39]. Several key placental genes that influence placental development and fetal osteogenesis (*Hgf*, *Kit1*, *IFN α 4*, *Ifrd*, and *IL-1 β*) are altered by methylnitrosourea and largely normalized by Q [39]. In this study, antioxidant effects of Q were noteworthy: our results showed that the GDM-induced placental OS and endothelial necrosis were significantly mitigated by Q supplementation. Results from this report also revealed that Q supplementation partially decreased maternal hyperglyce-

mia and hyperinsulinemia, and offer additional information about preventive and therapeutic management of GDM.

In conclusion, our data suggested that a diet high in saturated fat before and during pregnancy alters glucose metabolism and results in gestational hyperglycemia, development of insulin resistance, and placental OS. This novel method of GDM development in rodents may provide a useful tool for improving mechanistic understanding of OS and metabolic effects of HFD in GDM. Further study of maternal, fetal, and neonatal sequelae of this dietary intervention will offer more complete avenues for novel treatments and preventions of adverse consequences of GDM.

Acknowledgment

This research is supported by the Harvey W Peters Research Center Foundation.

References

- [1] Shao J, Yamashita H, Qiao L, et al. Phosphatidylinositol 3-kinase redistribution is associated with skeletal muscle insulin resistance in gestational diabetes mellitus. *Diabetes* 2002;51:19–29.
- [2] Lebovitz HE, Banerji MA. Treatment of insulin resistance in diabetes mellitus. *Eur J Pharmacol* 2004;490:135–46.
- [3] Saltiel AR, Olefsky JM. Thiazolidinediones in the treatment of insulin resistance and type II diabetes. *Diabetes* 1996;45:1661–9.
- [4] Bo S, Menato G, Lezo A, et al. Dietary fat and gestational hyperglycaemia. *Diabetologia* 2001;44:972–8.
- [5] Garcia-Patterson A, Erdozain L, Ginovart G, et al. In human gestational diabetes mellitus congenital malformations are related to pre-pregnancy body mass index and to severity of diabetes. *Diabetologia* 2004;47:509–14.
- [6] Rolo AP, Palmeira CM. Diabetes and mitochondrial function: role of hyperglycemia and oxidative stress. *Toxicol Appl Pharmacol* 2006;212:167–78.
- [7] Lyall F, Gibson JL, Greer IA, et al. Increased nitrotyrosine in the diabetic placenta: evidence for oxidative stress. *Diabetes Care* 1998;21:1753–8.
- [8] Paravicini TM, Touyz RM. Redox signaling in hypertension. *Cardiovasc Res* 2006;71:247–58.
- [9] Skibola CF, Smith MT. Potential health impacts of excessive flavonoid intake. *Free Radic Biol Med* 2000;29:375–83.
- [10] Holemans K, Caluwaerts S, Poston L, et al. Diet-induced obesity in the rat: a model for gestational diabetes mellitus. *Am J Obstet Gynecol* 2004;190:858–65.
- [11] Rerup CC. Drugs producing diabetes through damage of the insulin secreting cells. *Pharmacol Rev* 1970;22:485–518.
- [12] Aerts L, Sodoyez-Goffaux F, Sodoyez JC, et al. The diabetic intrauterine milieu has a long-lasting effect on insulin secretion by B cells and on insulin uptake by target tissues. *Am J Obstet Gynecol* 1988;159:1287–92.
- [13] Oh W, Gelardi NL, Cha CJ. Maternal hyperglycemia in pregnant rats: its effect on growth and carbohydrate metabolism in the offspring. *Metabolism* 1988;37:1146–51.
- [14] Oh W, Gelardi NL, Cha CJ. The cross-generation effect of neonatal macrosomia in rat pups of streptozotocin-induced diabetes. *Pediatr Res* 1991;29:606–10.
- [15] Luo J, Quan J, Tsai J, et al. Nongenetic mouse models of non-insulin-dependent diabetes mellitus. *Metabolism* 1998;47:663–8.
- [16] Widdowson PS. Obesity in diabetes and the impact of leptin. *Diabetes Rev Int* 1997;6:2–5.
- [17] Wilson BD, Ollmann MM, Barsh GS. The role of agouti-related protein in regulating body weight. *Mol Med Today* 1999;5:250–6.
- [18] Manach C, Morand C, Demigne C, et al. Bioavailability of rutin and quercetin in rats. *FEBS letters* 1997;409:12–6.
- [19] Reaven GM, Hollenbeck C, Jeng CY, et al. Measurement of plasma glucose, free fatty acid, lactate, and insulin for 24 h in patients with NIDDM. *Diabetes* 1988;37:1020–4.
- [20] Frayne KN. Insulin resistance and lipid metabolism. *Curr Opin Lipidol* 1993;4:197–204.
- [21] Steiner G, Morita S, Vranic M. Resistance to insulin but not to glucagon in lean human hypertriglyceridemics. *Diabetes* 1980;29:899–905.
- [22] Dresner A, Laurent D, Marcucci M, et al. Effects of free fatty acids on glucose transport and IRS-1-associated phosphatidylinositol 3-kinase activity. *J Clin Invest* 1999;103:253–9.
- [23] Belfiore F, Iannello S. Insulin resistance in obesity: metabolic mechanisms and measurement methods. *Mol Genet Metab* 1998;65:121–8.
- [24] Iwanishi M, Kobayashi M. Effect of pioglitazone on insulin receptors of skeletal muscles from high-fat-fed rats. *Metabolism* 1993;42:1017–21.
- [25] Rosholt MN, King PA, Horton ES. High-fat diet reduces glucose transporter responses to both insulin and exercise. *Am J Physiol* 1994;266:R95–R101.
- [26] Ohtsubo K, Takamatsu S, Minowa MT, et al. Dietary and genetic control of glucose transporter 2 glycosylation promotes insulin secretion in suppressing diabetes. *Cell* 2005;123:1307–21.
- [27] Djordjevic A, Spasic S, Jovanovic-Galovic A, et al. Oxidative stress in diabetic pregnancy: SOD, CAT and GSH-Px activity and lipid peroxidation products. *J Matern Fetal Neonatal Med* 2004;16:367–72.
- [28] Little RE, Gladen BC. Levels of lipid peroxides in uncomplicated pregnancy: a review of the literature. *Reprod Toxicol* 1999;13:347–52.
- [29] Myatt L, Kossenjans W, Sahay R, et al. Oxidative stress causes vascular dysfunction in the placenta. *J Matern Fetal Med* 2000;9:79–82.
- [30] Ottersbach K, Dzierzak E. The murine placenta contains hematopoietic stem cells within the vascular labyrinth region. *Dev Cell* 2005;8:377–87.
- [31] Blankenship TN, Enders AC. Expression of platelet-endothelial cell adhesion molecule-1 (PECAM) by macaque trophoblast cells during invasion of the spiral arteries. *Anat Rec* 1997;247:413–9.
- [32] Liang C, Oest ME, Jones JC, et al. Gestational high saturated fat diet alters C57BL/6 mouse perinatal skeletal formation. *Birth Defects Res B Dev Reprod Toxicol* 2009;86:362–9.
- [33] Prasad K, Daume E, Preuett B, et al. Glucagon is required for early insulin-positive differentiation in the developing mouse pancreas. *Diabetes* 2002;51:3229–36.
- [34] Liang C, Oest ME, Prater MR. Intrauterine exposure to high saturated fat diet elevates risk of adult-onset chronic diseases in C57BL/6 mice. *Birth Defects Res B Dev Reprod Toxicol* 2009;86:377–84.
- [35] Barker DJ. The fetal and infant origins of disease. *Eur J Clin Invest* 1995;25:457–63.
- [36] Pawlikowska-Pawlega B, Gruszecki WI, Misiak LE, et al. The study of the quercetin action on human erythrocyte membranes. *Biochem Pharmacol* 2003;66:605–12.
- [37] Paganga G, Rice-Evans CA. The identification of flavonoids as glycosides in human plasma. *FEBS Lett* 1997;401:78–82.
- [38] Hertog MG, Hollman PC. Potential health effects of the dietary flavonol quercetin. *Eur J Clin Nutr* 1996;50:63–71.
- [39] Prater MR, Laudermilch CL, Liang C, et al. Placental oxidative stress alters expression of murine osteogenic genes and impairs fetal skeletal formation. *Placenta* 2008;29:802–8.